

**Research  
paper**

# Development of new blasting technique for rescue work

Kana Nishino<sup>\*†</sup>, Shiro Kubota<sup>\*</sup>, Yuji Wada<sup>\*</sup>, Yuji Ogata<sup>\*</sup>, Norio Ito<sup>\*\*</sup>,  
Masayuki Nagano<sup>\*\*</sup>, Atsuya Fukuda<sup>\*\*\*</sup>, and Mieko Kumasaki<sup>\*\*\*\*</sup>

<sup>\*</sup>Research Institute of Science for Safety and Sustainability (RISS), National Institute of Advanced Industrial Science and Technology, 16-1 Onogawa, Tsukuba, Ibaraki, 305-8569, JAPAN

Phone : +81-29-861-8700

<sup>†</sup>Corresponding author : kana118-nishino@aist.go.jp

<sup>\*\*</sup>Sagami Kogyo Co., Ltd., 1-3-12 Yoshinodai, Chuo-ku, Sagamihara, Kanagawa, 252-0222, JAPAN

<sup>\*\*\*</sup>Kayaku Japan Co., Ltd., KFC Bldg. 9F, 1-6-1 Yokoami, Sumida-ku, Tokyo, 130-0015, JAPAN

<sup>\*\*\*\*</sup>Yokohama National University, 79-7 Tokiwadai, Hodogaya-ku, Yokohama, Kanagawa, 240-8501, JAPAN

Received : August 31, 2015 Accepted : January 29, 2016

## Abstract

In order to rescue trapped victims in a collapsed building, a new breaching technique that supports rescue operation was developed. The breaching technique employs explosives to partially destroy a reinforced concrete (RC) wall. This paper reports experimental results of RC walls which has a thickness of 150 mm. Single-charge experiments provided two types of fracture manner depending on the position of explosive center. Based on the results of the single-charge experiments, partial-charge and full-charge experiments were carried out at the charge conditions considered to be suitable for this new breaching technique. As a result, the optimal charge condition was found. The fracture processes were discussed by means of high-speed photography.

**Keywords** : breaching, reinforced concrete (RC) wall, explosive center, fracture processes

---

---

## 1. Introduction

When an earthquake occurs, people can be trapped collapsed buildings. As for the great earthquake in Japan in 1995, many people suffered crush injuries, and people were less alert to them. Earthquake victims have to be rescued from the area as soon as possible, since the survival rate of victims drop dramatically unless they rapidly receive proper treatment<sup>1)</sup>. Immediate treatment is essential for people trapped within difficult to move debris. However, the broken walls and ceilings can block access routes for rescue crews trying to reach the entrapped victims.

One of the techniques to solve the problem is breaching<sup>2)</sup>, which opens a space in a remaining reinforced concrete (RC) wall or floor. The procedure consists of three phases: survey the condition, open a hole, and remove the reinforcing bars. The hole enables rescuers to

enter the confined space and save victims. On the other hand, it has some problems. The current breaching methods take time to open a route for rescuers and generate fine dust. This poses health risks to the rescue crews. The equipment itself is large and heavy, and requires large and heavy batteries as a source of electricity. Additionally, damaged and disrupted transportation hinders rescuers from carrying them in the midst of the chaos surrounding the disaster.

In order to overcome the problems of the current methods, we have applied explosives to breach RC walls<sup>3)-5)</sup>. Our new method requires explosives, a rotary hammer drill, an explosives ignition switch, stemming and relating cables. They are light enough to carry to the area where rescue activities are needed. The new breaching process involves surveying the conditions, drilling holes for explosives, placing explosives, locking the holes with

stemming, connecting cables, and igniting the explosives. Each process reduces exposure time that poses a risk for rescue crews as compared with the breaching methods using a saw. The methods are considered promising and need further development for practical use.

Explosives have been widely used for demolishing large buildings or shaping lands. Such big projects require large amount of explosives with enough power to accomplish them. On the other hand, detonations with small explosive charges were employed for controlled local demolitions. Blasting by using a small explosive charge was presented as economically attractive<sup>6)</sup>. The small explosive charge was also preferred over high detonating explosives, and the explosives were used in small charges, (e.g., 10 g per charge), along with a small diameter borehole of approximately 10-18 mm<sup>7)</sup>. Molin and Laurizen explained the experimental condition<sup>8)-11)</sup>. Although this method was not invented for breaching, it was suitable for this purpose because it was possible to create partial fractures, and the blasting procedure, along with the blasting vibration, and the noise, were reduced<sup>12)</sup>.

To maximize the benefit of the blasting by using a small explosive charge, this study aims at utilizing the technique for breaching in order to rescue victims. The promotion of the technique requires a defined relationship between the charge conditions and the size of the crater left after detonation, such as its depth and diameter. The relationship can be obtained by experiments with RC structures. The experiment will provide the proper charge conditions in order to control explosion energy for fracturing a necessary and sufficient area of a wall for rescuers, taking into consideration, the amount of explosives directly influencing the blast, the amount of dust generated, and flying debris which are harmful to them. The optimized amount of explosives is essential for the practical use of this method, as the borehole depth affects the victims as well as rescue crews. The breaching techniques can be divided into two types in terms of destruction on the other side of which rescue crews work. "Clean" breaching prevents the fragments spreading behind the wall. "Dirty" breaching denotes the technique allowing the fragments to scatter on the victims' side. Deeper holes tend to cause dirty breaching.

This article focuses on the effects of the borehole depth and the amount of explosives. Various parameters, such as angles and diameters of borehole, affect the amount of RC removed in breaching. However, this study investigates the amount of explosives used and the borehole depth, for prioritizing the safety of rescue crews.

## 2. Experiment

### 2.1 Sample of RC wall

The density of the sample was 2300 kg/m<sup>3</sup>. The steel rods used to reinforce concrete were 13 mm in diameter and were placed in a grid pattern in the middle of the wall. The size and arrangement of the steel rods in the wall are described in Figure 1. The thickness of the sample of RC wall was 150 mm. Our survey of demolished buildings and interviews of wreckers found that the thickness of walls

are commonly 150 mm. Two types of RC walls were prepared as samples whose width and height were 1000 mm and 1500 mm, respectively. The uniaxial concrete compressive strengths used were 31.3 MPa, 22.3 MPa and 27.7 MPa.

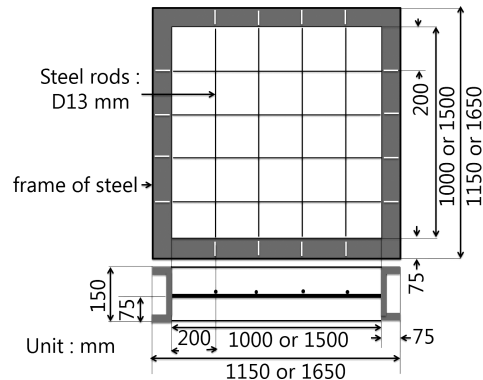


Figure 1 Sample of reinforced concrete (RC) wall.

### 2.2 Charge conditions

Figure 2 shows the prototype of the explosives device. The device itself is 3.0 g and consists of 2.6 g C-4 explosive and a No.6 electric detonator. The detonator contains 0.4 g of a base charge. The total amount of explosives in the device was adjusted by the amount of the C-4 explosives. The outer diameter is 13 mm, and the total length of the device is only 60 mm for the 3.0 g case. The amount of C-4 and the length of the explosives device are shown in Table 1.

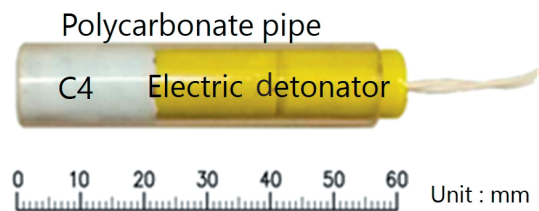


Figure 2 Explosive device.

Table 1 Amount of C4 explosive and length of explosive device.

| Amount of C4 [g] | Length of C4 [mm] | Length of device [mm] |
|------------------|-------------------|-----------------------|
| 2.0              | 13.0              | 55.0                  |
| 2.5              | 16.0              | 57.0                  |
| 3.0              | 20.0              | 60.0                  |
| 3.5              | 24.0              | 65.0                  |

Each borehole was drilled to a planned depth prior to charging to ensure each explosives device was placed completely in the wall and the stemming was locked in the borehole effectively. Boreholes were drilled vertically into the wall, and clay was used as a stemming material. The designed borehole in these experiments was small compared with ordinary blasting, because of the small diameter of explosives device. The diameter of the borehole was 16 mm.

Figure 3 shows the setting for the full-charge experiment. The holes were spaced in triangular shape where all sides had an equal length of 900 mm, and the distance between boreholes was fixed at 180 mm. The concrete for triangle part has to be removed to pass the

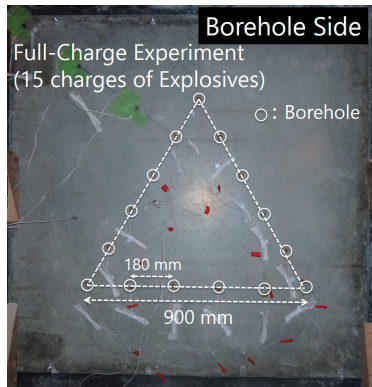


Figure 3 Setting for the full-charge experiment.

stretcher.

Single-charge experiments were carried out to obtain the relationship between crater size and explosives charge. The practical effect of the proposed blasting technique on the breaching was estimated by partial-charge experiments as shown in Figure 4. Based on the result of the partial-charge experiment, the borehole depth and the amount of explosive for the full-charge experiment were determined. The full-charge experiments were conducted to examine the fracture condition of 15 charges used to open the entire triangular space.

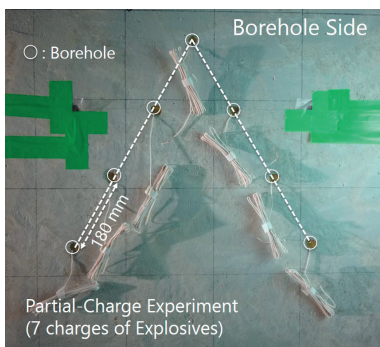


Figure 4 Setting for the partial-charge experiment.

### 2.3 Measurement

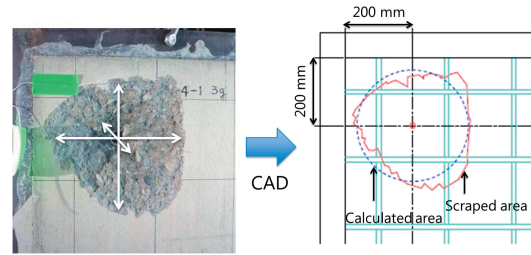
High-speed photography using FASTCAM-SA 5 (Photron Ltd.) was employed to observe the fracture process of the crater.

The results of blasting were used to evaluate crater sizes. The example of the crater is shown in Figure 5. The crater profiles were generated using measurements of the vertical and horizontal size and depth. The results of each blasting were stored as photo images. The image data were processed with AutoCAD (Autodesk, Inc.) to calculate the scraped area. A radius was calculated from a circle whose area was the same as the scraped area.

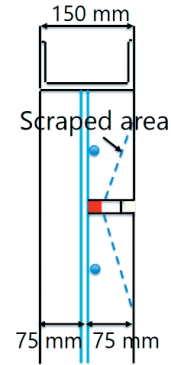
## 3. Results and discussion

### 3.1 Single-charge experiments

The typical fracture manner is shown in Figure 6. The amount of explosives was fixed at 3.0 g, and the borehole depth was varied from 75 mm to 90 mm at intervals of 5 mm. Two types of fracture conditions were confirmed. Type A is shown in Figure 6 (a), (b), (c), and (d). The crater was generated only on the borehole side, and the



(a) Borehole-section.



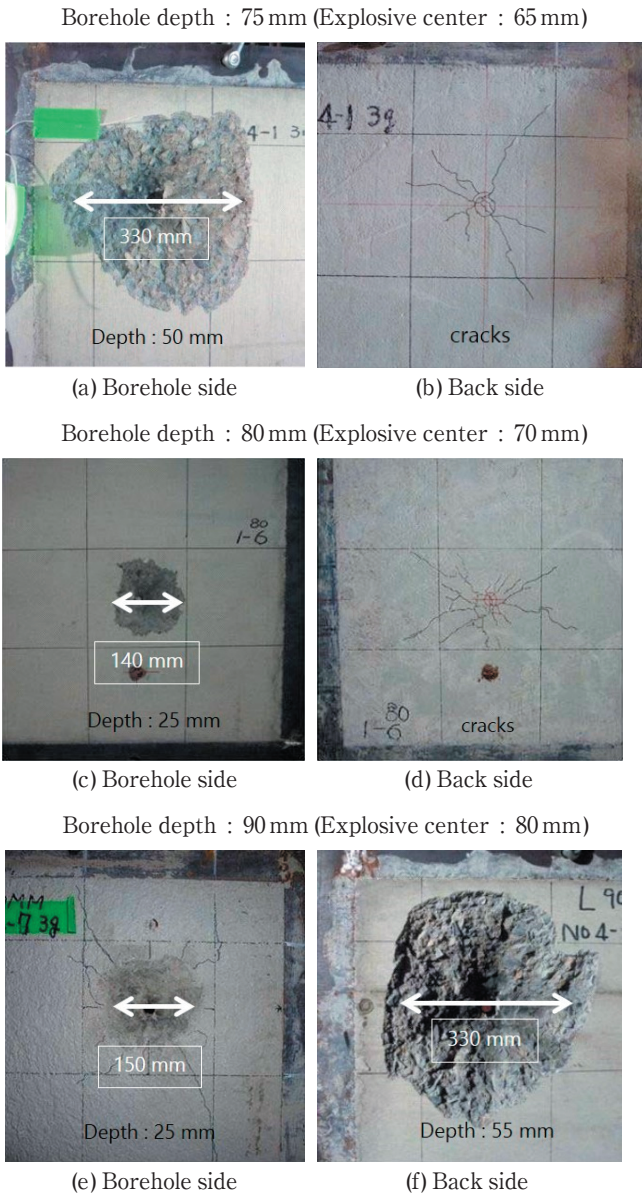
(b) Cross-section.

Figure 5 Example of the crater.

back side contained only cracks. This fracture manner is suitable for clean breaching. Type B is shown in Figure 6 (e) and (f), where craters were generated on both sides. This fracture manner may be suitable for dirty breaching. In the experiments, the surface with the borehole opened is called the “borehole side” and the other surface is the “back side.” The fracture conditions depend on the position of the explosive center. “Explosive center” is the position of the center of explosives. The length of C-4 explosives at 3.0 g was 20 mm. The explosive center was 10 mm away from the bottom of borehole depth.

The fracture manner was Type A when the explosive center was positioned between the borehole side and the middle of the wall. The exact middle point of the walls is not included in the region. When the borehole depth was 75 mm, a crater with a 50 mm depth and 330 mm diameter was generated as shown in Figure 6 (a) and (b). The result of the 80 mm borehole depth is shown in Figure 6 (c) and (d). The depth of the crater was 25 mm. The crater was smaller than the one created using a borehole depth of 75 mm. The difference in crater size is remarkable, as shown in Figure 6 (a) and (c). Although the difference between the 75 mm and 80 mm borehole depth is only 5 mm, the difference of the crater size at the borehole side was confirmed. Under experimental conditions, it can be considered that a 75 mm borehole depth is an optimal condition for clean breaching.

The 90 mm borehole depth created a Type B fracture condition, as shown in Figure 6 (e) and (f). In this case, the explosive center was beyond the middle of the wall. The depth and diameter of the crater on the borehole side were 25 mm and 150 mm, respectively. On the back side, the depth was 55 mm, and the diameter was 330 mm. The sum of the crater depths at the borehole side and back side was 80 mm. The total depth of the crater for Type B is



**Figure 6** Fracture manner of Type A and Type B. Result of the single-charge experiments. Type A : (a), (b), (c), and (d) Type B : (e) and (f)

larger than that for Type A. RC walls with a concrete compressive strength of 22.3 MPa and 31.3 MPa were used for the above-mentioned experiments. The relationship between the fracture manners and the position of the explosive center did not depend on the differences of compressive strength of concrete had no obvious impact on the relationship between the fracture manners and the position of the explosive center.

When the explosive center was located at the middle of the RC wall, the fracture manner depended on the concrete compressive strength. In the case of the 85 mm borehole depth, when the compressive strength of sample was 22.3 MPa, the crater was generated only on the borehole side as in Figure 7 (a) and (b). On the other hand, when the compressive strength of sample was 31.3 MPa, the crater was generated on both sides as in Figure 7 (c) and (d).

Using high-speed photography, it was found that the product gas ejects from the borehole before the

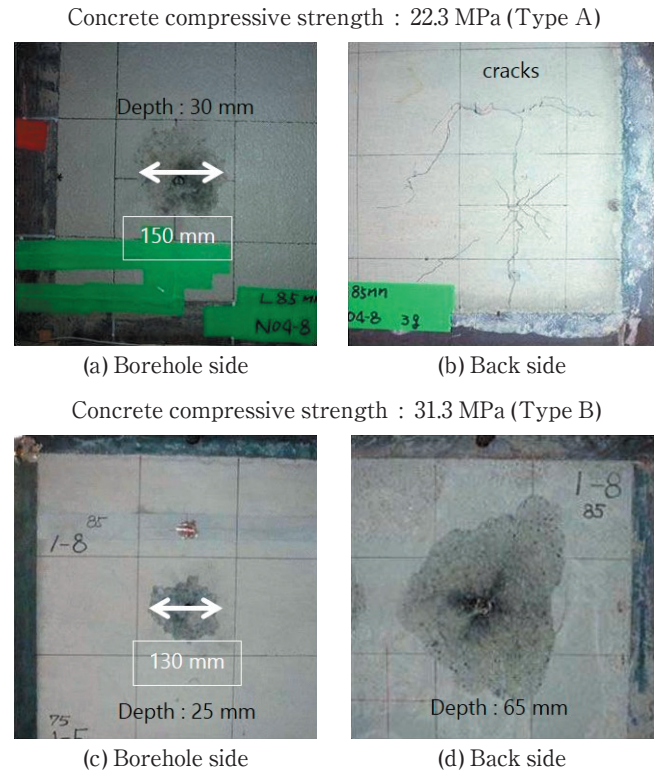


**Figure 7** Fracture manner of the 85 mm borehole depth (75 mm explosive center). Result of the single-charge experiments.

generation of the crater at both sides of the wall. The fragmentation at the surface of the borehole side is generated faster than that of the back side. We considered the fragmentation at the borehole side. In the experiment as shown in Figure 7 (a), since the concrete compressive strength is lower than that in the case of Figure 7 (c), more of the product gas than in the case of Figure 7 (c) was ejected from the borehole side. As a result, the explosion energy needed to generate the crater at the back side was decreased compared with the case shown in Figure 7 (d), so the crater was not generated at the back side.

The relationship between the amount of explosives and the depth of the crater with a fixed borehole depth is shown in Figure 8. Figure 8 (a) is the case of the 75 mm borehole depth, and (b) and (c) are the case of the 90 mm borehole depth. The amount of explosives were 2.0, 2.5, 3.0, or 3.5 g.

In case of the 75 mm borehole depth, the crater was generated only on the borehole side, regardless of the amount of explosives. The depth of the crater did not change with the exception of the experiment with 2.0 g. The depth of the crater caused by 2.0 g was shorter than the others as shown in Figure 8 (a).

In the case of the 90 mm borehole depth, the craters were always generated in the back side regardless of the amount of explosives as shown in Figure 8 (c). The depth of the crater on the back side was almost the same, regardless of the amount of explosives. However, the crater generation on the borehole side was influenced by the amount of explosives as shown in Figure 8 (b). The results from 2.0 g of explosives showed that the no crater generation occurred. When the amount of explosives was

3.5 g, the depth of crater generated on the borehole side was deeper than the others. If a crater would need to be generated on the borehole side or both sides, the amount of explosives would need to be more than 2.5 g.

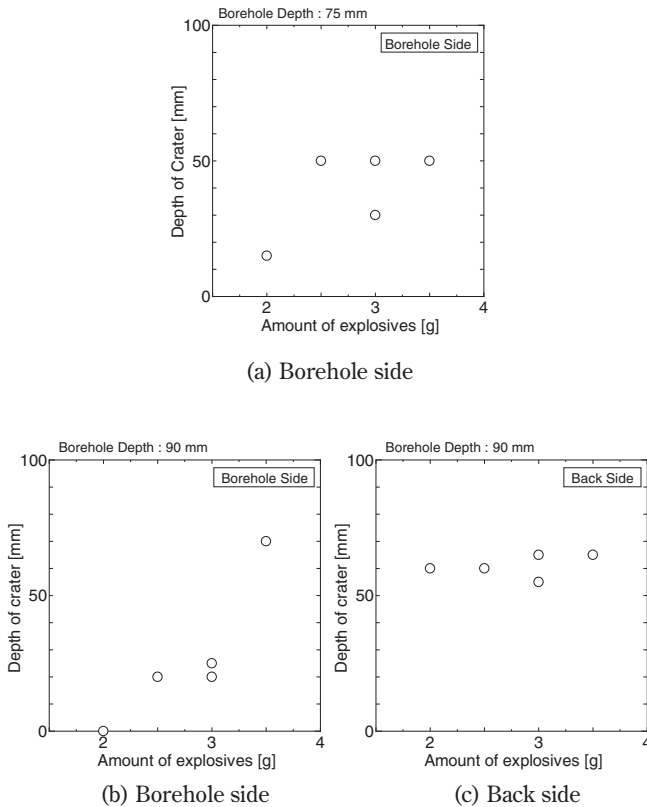


**Figure 8** Relationship between the amount of explosive and the depth of crater.

### 3.2 Partial-charge and full-charge experiments

In the case of the 75 mm borehole depth, partial-charge and full-charge experiments were conducted with 2.5 g/hole and 3.0 g/hole of explosives, in order to confirm the crater was generated only on borehole side. Also, in the case of the 90 mm borehole depth, the experiments with partial-charge and full-charge experiments were conducted with 3.0 g/hole and 3.5 g/hole of explosives, in order to confirm the craters were generated on both sides. The fracture manner in partial-charge is shown in Figure 9.

In the case of the 75 mm borehole depth with the 3.0 g of explosives, the crater was generated only on the borehole side, and the cracks expanded to form a triangle on the back side as shown in Figure 9 (a) and (b), respectively. The similar results were obtained in other experiments of the 75 mm borehole depth regardless of the amount of explosives.

In the case of the 90 mm borehole depth, the crater was generated on both sides as shown in Figure 9 (c) and (d) regardless of the amount of explosives. The partial-charge and full-charge experiments showed the same relationship as the single-charge experiment.

The relationship between the concrete compressive strength and the depth of the crater is shown in Figure 10.

In case that the amount of explosive was 3.0 g, the average depth of the crater was similar between 75 mm and 90 mm borehole depth regardless of the concrete

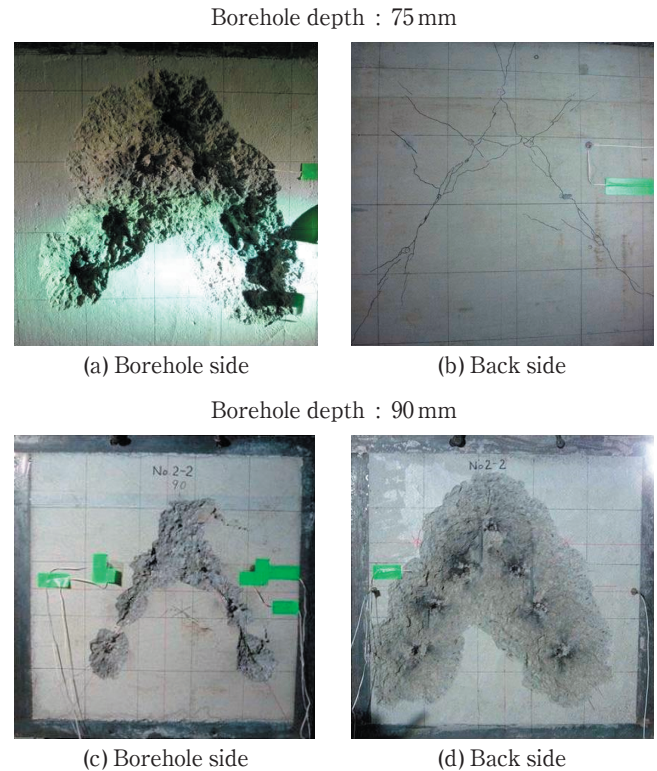


**Figure 9** Fracture manner of partial-charge experiment.  
Charge condition : 3.0 g/hole  
(a) and (b) : 75 mm borehole depth  
(c) and (d) : 90 mm borehole depth

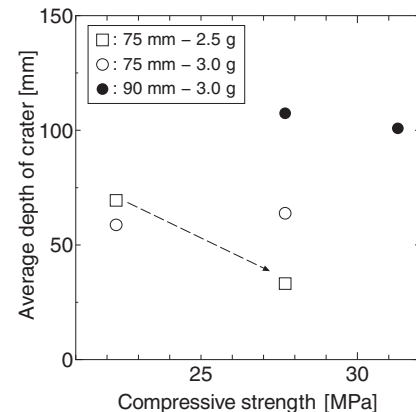


**Figure 10** Relationship between the concrete compressive strength and the depth of crater.

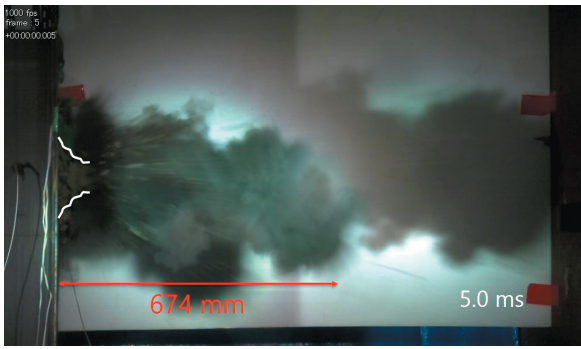
Results of the partial-charge and the full-charge experiments.

compressive strength as shown in Figure 10. On the other hand, in case of 2.5 g of explosive, the average of depth of the craters was affected by the concrete compressive strength as is shown in Figure 10.

This new breaching technique is expected to be used for rescue work in a disaster, where rescue crews need to combat any type of destroyed walls. Therefore, it can be considered that the charge condition should not be influenced by the concrete compressive strength. In that sense, the 75 mm borehole depth with the 3.0 g of explosive is the optimal condition for clean breaching of 150 mm thick RC wall.

### 3.3 Fracture processes

The fracture processes of the crater generated on the



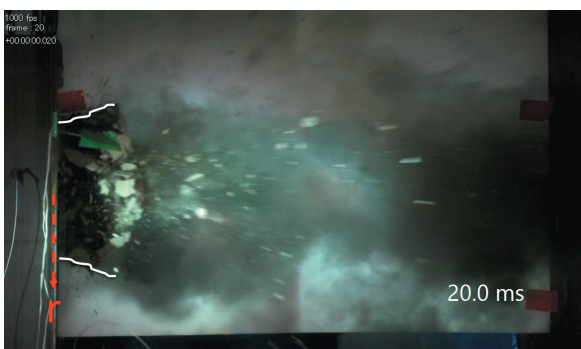
(a) After 5.0 milliseconds.



(b) After 10.0 milliseconds.



(c) After 15.0 milliseconds.



(d) After 20.0 milliseconds.

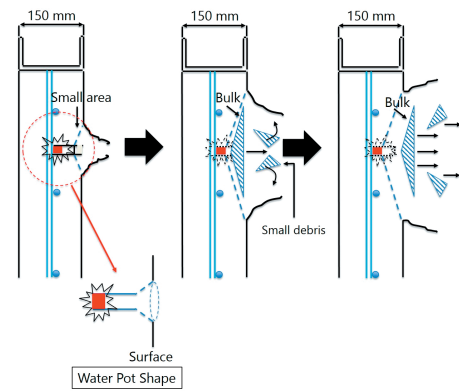
**Figure 11** Fracture processes at the borehole side obtained by high-speed photography.  
(Type A)  
Borehole depth : 75 mm (Explosive center : 65 mm)  
Time is counted after explosion. The speed : 1,000 fps  
Diameter of crater : 330 mm (Depth of crater : 50 mm)

borehole side and the back side are discussed here. Figure 11 shows the fracture process obtained by high-speed photography on the borehole side. The white lines in Figure 11 show the shape of the fractured wall, and those lines indicate the motion of the fractured wall. Five

milliseconds after the explosion, the fractured wall rises intensively only near the borehole location, as shown in Figure 11 (a). At this time, it was confirmed that the explosion gas jetted from the surface of the wall to a distance of 674mm. Based on the Figure 11, the fracture processes at the borehole sides can be considered as follows :

The conceptual diagram for the fracture processes at the borehole side is shown in Figure 12. A small amount of explosive generates a water pot shape fracture as shown in Figure 12 (a). The crater shown in Figure 6 (c) is this type of fracture. When the amount of explosive increase, the fracture near the free surface with the water pot shape occurs, at the same time, other fracture with the size of the diameter of the crater also generate as shown in Figure 12 (b). The fragment with the size of diameter of the crater spalls, then it moves. The fracture process proceeds as follows as shown in Figure 12 (c).

In contrast, the fracture processes on the back side shown in Figure 13 can be considered as follows :



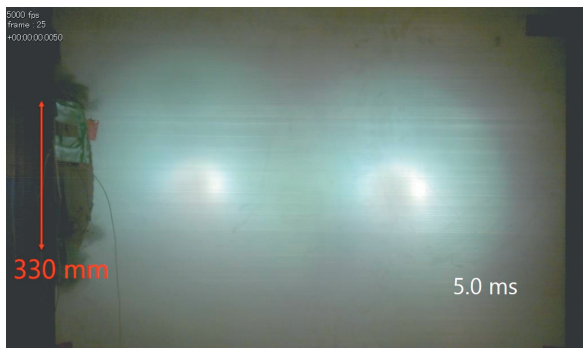
(a) First step (b) Second step (c) Completion

**Figure 12** Fracture process at the borehole side.

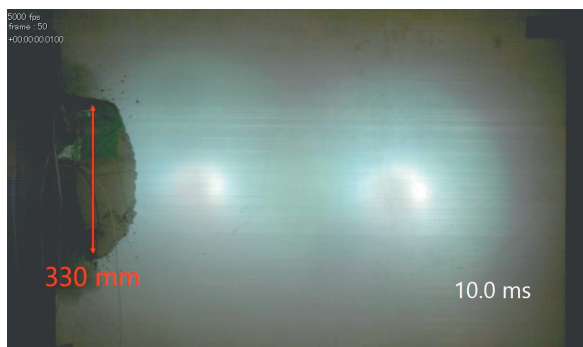
The conceptual diagram for fracture processes at the back side is shown in Figure 14. The surface of the wall spalls at the range of the diameter of the crater as shown in Figure 14 (a) and (b). The spalled fragments move without any velocity distribution. Finally, the spalls fracture causes debris as shown in Figure 14 (c).

#### 4. Conclusion

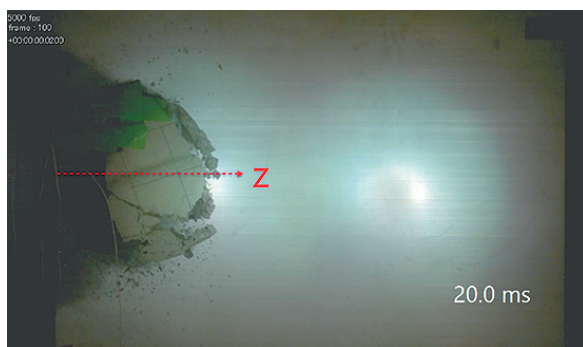
Aiming at rescue work in a disaster, a new breaching technique was developed. Experiments were carried out on a RC wall with 150 mm thick RC wall. Single-charge experiments were conducted with 3.0 g of explosives. The borehole depth was increased stepwise by 5 mm from 75 mm up to 90 mm. In these experiments, two types of fracture conditions were observed depending on the position of the explosive center. When the explosive center was at the borehole side, the crater generated only on borehole side. When the explosive center was at between the middle of the wall and the back side, the crater generated in both sides. The relationship between the fracture manners and the position of the explosive center was independent from the concrete compressive strength. When the explosive center was located at the middle of the RC wall, the fracture manner depended on



(a) After 5.0 milliseconds.



(b) After 10.0 milliseconds.



(c) After 20.0 milliseconds.

**Figure 13** Fracture processes at the back side obtained by high-speed photography.

(Type B)

Borehole depth : 90 mm (Explosive center : 80 mm)

Time is counted after explosion. The speed : 5,000 fps

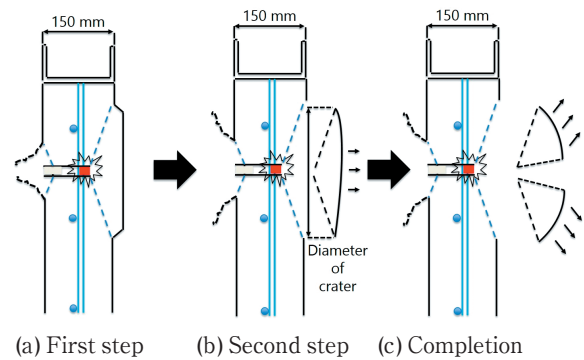
Diameter of crater : 330 mm (Depth of crater : 55 mm)

the concrete compressive strength.

Under the condition of the fixed borehole depth, experiments were conducted with 2.0, 2.5, 3.0 and 3.5 g of explosives. 2.0 g of explosives generated the no crater. If breaching needs to generate an effective crater on the borehole side or both sides, the amount of explosives should be more than 2.5 g.

Based on the results of the single-charge experiments, the partial-charge experiment and full-charge experiment were carried out under the charge condition which is considered to be suitable for new breaching. As a result, the optimal charge condition was found.

The fracture processes were discussed on the basis of the high-speed photography. The fracture process at the back side, the fractured wall moves at the range of the diameter of the crater.



(a) First step (b) Second step (c) Completion

**Figure 14** Fracture process at the back side.

This paper represents the optimal condition for breaching based on the experiments. The results are expected to contribute to providing an option for rescue work in a disaster.

### Acknowledgment

This study was supported by the Promotion Program for Scientific Fire and Disaster Prevention Technologies in 2012 and 2013.

### References

- 1) N. Yoshimura, S. Nakayama, K. Nakagiri, T. Azami, K. Ataka, and N. Ishii, *Chest*, 110, 3, 759–761 (1996).
- 2) FEMA NATIONAL US&R RESPONSE SYSTEM Structural Collapse Technician 02–00, Module 3 — Breaching-Breaking-Cutting-Burning, 13–17 (1999).
- 3) S. Kubota, K. Nishino, Y. Wada, Y. Ogata, N. Ito, M. Nagano, S. Nakamura, T. Taguchi, and A. Fukuda, *Proc. The 7th International Conference on Explosives and Blasting*, 235–240, Metallurgical Industry Press (2013).
- 4) K. Nishino, S. Kubota, Y. Wada, Y. Ogata, N. Ito, M. Nagano, S. Nakamura, T. Taguchi, and A. Fukuda, *Explosion, Shock Wave and High-Energy Reaction Phenomena 2*, Materials Science Forum 767, 154–159 (2014).
- 5) K. Nishino, S. Kubota, Y. Wada, Y. Ogata, N. Ito, M. Nagano, S. Nakamura, T. Taguchi, and A. Fukuda, *Proc. The 8-th International Symposium on Impact Engineering*, 268–273, *Applied Mechanics and Materials* 566 (2014).
- 6) J. Schneider, *Proc. The second Int. RILEM symposium*, 88–97, *Demolition Methods and Practice* (1988).
- 7) E.K. Lauritzen, *Proc. The second Int. RILEM symposium*, 49–58, *Demolition Methods and Practice* (1988).
- 8) C. Molin, “Localized cutting in concrete with careful blasting —Full-scale experiments in an old concrete building with a comparison of methods-”, *Swedish Cement and Concrete Research Institute*, 252 (1983).
- 9) C. Molin, “A methods development study of localized cutting in concrete with careful blasting”, *Swedish Cement and Concrete Research Institute*, 149 (1984).
- 10) E. K. Lauritzen, *Building and Practice*, 14, 274 (1986).
- 11) C. Molin, *Proc. The second Int. RILEM symposium*, 69–78, *Demolition Methods and Practice* (1988).
- 12) Y. Ogata, “Practical application and popularization of mini-blasting considered with environment”, *Explosion, Journal of the Japan Explosive Society*, 18, 151–154, (2008) (in Japanese).